

Generation of a continuous-wave pulse train at a repetition rate of 17.6 THz

Shin-ichi Zaitzu, Chihiro Eshima, and Kazuki Ihara

Graduate School of Engineering, Kyushu University, 744 Motooka, Nishi-ku, Fukuoka 819-0395, Japan

Totaro Imasaka

Graduate School of Engineering, and Center for Future Chemistry, Kyushu University, 744 Motooka, Nishi-ku, Fukuoka 819-0395, Japan

Received November 11, 2006; revised January 15, 2007; accepted January 19, 2007;
posted January 29, 2007 (Doc. ID 76852); published April 17, 2007

We demonstrated that a 17.6 THz pulselike intensity modulation resulted from the coherent superposition of multifrequency continuous-wave emissions generated from a hydrogen-filled high-finesse cavity through a cascade-stimulated Raman scattering process. We pointed out that the complete phase-locked operation was hindered by the intracavity dispersion that caused nonequal separations between adjacent emission lines.

© 2007 Optical Society of America

OCIS codes: 140.3550, 320.7090, 140.4050.

1. INTRODUCTION

Fourier synthesis of equally separated laser emissions provides a train of pulses whose repetition rate corresponds to the frequency separation between the emission lines. Hence a pulse train operated at a terahertz (THz) repetition rate in the continuous-wave (CW) mode can be generated by synthesizing phase-locked multiple-line CW laser emissions with a frequency separation larger than a THz. Such a CW-based THz pulse train is required to generate a narrow-linewidth THz radiation for biomolecular imaging,¹ ultrahigh-capacity communications,² and an optical clock in all-optical data processing.³ Several schemes to obtain a CW-THz pulse train have been proposed: harmonics mode locking in a semiconductor laser,^{4,5} synthesis of emissions from multiple phase-locked lasers,⁶ and beat-soliton conversion through an optical fiber with high nonlinearity.⁷ However, repetition rates achieved by these techniques are limited to a few THz due to the limitation of the bandwidth of a gain medium or anomalous dispersion in a fiber.

An alternative method to increase the repetition rate, based on Fourier synthesis of high-order stimulated Raman emissions with an equal frequency separation, has been studied theoretically⁸ and experimentally.^{9,10} Harris and coworkers reported⁹ the generation of a nearly 100 THz pulse train, with a duration of less than 1.6 fs, by means of Fourier synthesis of the high-order stimulated Raman emissions arising from deuterium pumped by two-color transform-limited nanosecond laser pulses. Katsuragawa *et al.* generated a train of femtosecond pulses with a peak intensity of 2 MW level at a repetition rate of 10.6 THz using *para*-hydrogen as a Raman medium,¹⁰ based on the principle similar to that of Harris and coworkers.⁹ In this approach, although the pulse train is highly stable, the pulses are limited to inside the envelope of the pump pulse that has a duration of about several

nanoseconds, since a pair of high-peak-power nanosecond pump pulses are necessary to sufficiently excite Raman coherence for the molecules. Therefore this approach has difficulty using a low-power CW laser as a pump source for the generation of a THz pulse train in a CW mode that will be useful for some of the applications mentioned in the preceding paragraph.

In this paper, we experimentally demonstrate what is to our knowledge a novel approach to generate a CW-based THz pulse train operated at a repetition rate above 10 THz. This approach is based on coherent superposition of CW rotational Raman emissions generated from a high-finesse optical cavity containing a gaseous Raman-active medium.¹¹ In this approach, we first observed high-order stimulated Raman scattering (SRS) using a CW near-infrared single-frequency laser as a pump source. Next, we measured a waveform synthesized by coherent superposition of these CW Raman emissions by means of a highly sensitive autocorrelator based on two-photon absorption of a photocathode in a photomultiplier. We observed intensity modulation at a frequency of 17.6 THz, which corresponds to the rotational Raman shift frequency of *ortho*-hydrogen, although the emission lines were not completely phase locked due to nonequal frequency separations between the longitudinal modes of the high-finesse cavity caused by a dispersion arising from the gaseous hydrogen used as a Raman medium. Nevertheless, this result suggests the potential that this method has for the generation of a stable CW-THz pulse train synthesized by phase-locking multifrequency emissions when a high-finesse dispersion-controlled optical cavity is used as the CW Raman emission generator.

2. EXPERIMENT

The experimental setup is similar to one previously reported¹² for the generation of high-frequency

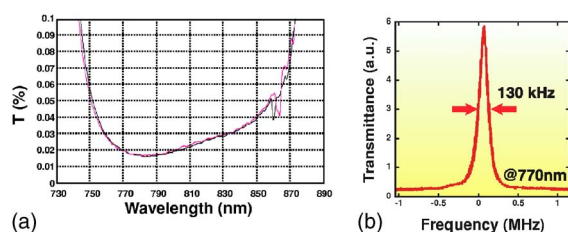


Fig. 1. (Color online) (a) Transmission spectrum of cavity mirrors. The incident angle is normal to the surface. (b) Transmission spectrum of the cavity. The wavelength of the input laser is 770.0 nm. The instantaneous linewidth of the input laser is sufficiently small (<10 kHz).

sinusoidal-modulated CW emission, which includes a high-finesse optical cavity, optics and electronics for a feedback control of the cavity, and a pump laser source. The design is essentially based on the instrument developed by Carlsten and coworkers for CW Raman lasing.¹³ A broadband high-finesse cavity with two concave mirrors ($r=250$ mm) with the same reflective property [see Fig. 1(a)] was specially designed and used in this experiment. The cavity was installed in a chamber filled with gaseous hydrogen at a pressure of 10 atm. A piezoelectric transducer was used as an actuator, with a maximum stroke of $5\text{ }\mu\text{m}$, and was attached to one of the mirrors to change the distance between the two mirrors (~ 8 cm) with nanometer-level precision. The cavity was controlled by the standard Pound–Drever–Hall (PDH) method to maintain a resonant condition of the cavity against the frequency of the pump laser. A narrow-linewidth Ti:sapphire laser (Coherent, MBR110) emitting at a wavelength of 770.0 nm was used as a pump source for multifrequency CW Raman lasing. The polarization of the beam was changed by passing it through a quarter-wave plate before focusing it into the cavity with mode-matching optics. The laser power measured at a position just before the cavity was about 200 mW.

The reflective property of the cavity mirrors [see Fig. 1(a)] shows that the mirrors have a reflectivity of $\geq 99.96\%$ over a frequency range of 44 THz. This broad bandwidth in the reflectivity of the cavity mirrors allows simultaneous resonance of the pump and two rotational Raman emissions arising from *ortho*-hydrogen, whose Raman shift frequency is 17.6 THz (586.9 cm^{-1}) under high-finesse ($\sim 10^4$) conditions. When the wavelength of the pump laser is adjusted to 770.0 nm, the finesse can be estimated to be $\sim 1.6 \times 10^4$ at the pump wavelength, $\sim 1.5 \times 10^4$ at the first Stokes emission, and $\sim 9 \times 10^3$ at the second Stokes emission. In fact, the linewidth of the cavity, measured by the transmission power while changing the cavity length at the wavelength of 770.0 nm, was 130 kHz [see Fig. 1(b)]. This is in good agreement with the value calculated from the reflectivity shown in Fig. 1(a).

Spectra were measured with a multichannel spectrometer (Ocean Optics, USB2000). The temporal waveform of the CW-based pulse train arising from the cavity was characterized using a standard interferometric autocorrelation (AC) method. However, since the peak power of the output beam was relatively small (~ 10 mW), the autocorrelator required a highly sensitive detector with a nonlinear response to obtain a second-order autocorrelation

trace. Hence we used a photomultiplier (Hamamatsu, 1P28) with a Sb–Cs photocathode that had a two-photon response rather than a one-photon response in the near-infrared region. This type of autocorrelator has been used elsewhere for the characterization of mode-locked laser pulses at an averaged power below 1 mW.¹⁴

3. RESULTS AND DISCUSSION

When the system was properly aligned, we observed the beam profile of a TEM_{00} single transverse mode for an output beam emitting from the Raman cavity. In this case, the measured spectrum included three emission lines with comparable intensities [see Fig. 2(a)]. The frequency separations between a couple of adjacent lines was 17.6 THz, which corresponds to the rotational Raman shift frequency for *ortho*-hydrogen. Thus these three lines can be assigned to the pump (P: 770.0 nm), the first (S1: 806.5 nm), and the second (S2: 846.5 nm) rotational Stokes emissions, respectively. The near-field beam profile was measured after separation of the beam using a diffraction grating, showing a TEM_{00} Gaussian mode for all the emission lines [see Fig. 2(b)]. It is well known that the beam profile of a high-order Stokes emission often exhibits a ring shape due to limitations in phase matching for four-wave mixing (FWM).¹⁵ In the present results, however, the profile of S2 shows a TEM_{00} mode that is the same as that of P and S1, suggesting that the generation of the S2 emission was not through a FWM process but through a cascade SRS process. This would also be supported by the fact that the maximum power of S2 was obtained using a circularly polarized pump beam; it should be noted that the rotational SRS is most efficient when the pump beam is circularly polarized.¹⁶

This is, to our knowledge, the first observation of high-order CW Stokes emissions from a nonresonantly pumped Raman medium. The threshold of SRS for a medium in a high-finesse cavity is substantially reduced by the resonant enhancement at both frequencies for the pump beam and for the seed component of the Stokes emission.¹³ In

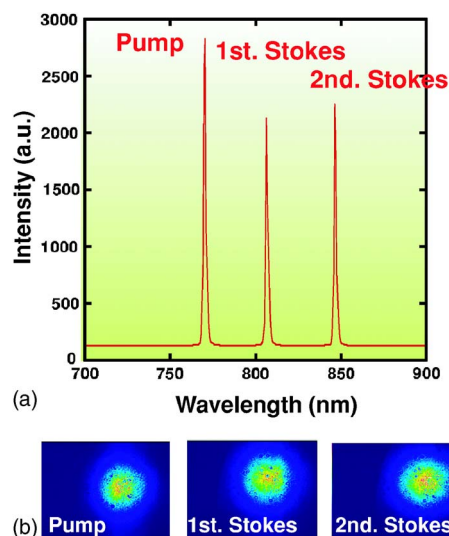


Fig. 2. (Color online) (a) Spectrum of an output beam from the Raman cavity. (b) Near-field patterns of the output pump, first Stokes, and second Stokes beams.

our broadband high-finesse cavity, both of the seed components for S1 and S2 are strongly enhanced, allowing the use of a CW laser with hundreds of milliwatt levels for the efficient generation of S2 emission. Moreover, we observed the generation of third Stokes emission (S3: 890.8 nm) when we measured an output spectrum after a monochromator tuned to the wavelength of S3. Unfortunately, we were not able to measure the power of S3 since it was smaller than the intensity of stray light from the pump emission in our monochromator. This faint intensity of S3 would be caused by the fact that the wavelength was out of range for the high-finesse region of our cavity. However, this result suggests that an expansion of the high-finesse region will lead to the strong enhancement of the higher-order Stokes emission even at the present pump power level (approximately hundreds of milliwatts). It should also be noted that the first anti-Stokes emission (AS1: 736.7 nm) was also observed using a monochromator, although the power of it was also extremely weak. This indicates that a FWM process generating the AS1 emission through an interaction between P and S1 occurred in the cavity, even though FWM requires a phase-matched condition for efficient generation. This would be caused by phase matching in a nearly collinear geometry due to the relatively small dispersion of the gaseous Raman-active medium.

The total output power of the emissions from the cavity was around 25 mW. Possible explanations for the power loss are (1) backward scattering of Stokes emission and backreflection of the pump beam,¹⁷ (2) light absorption by the cavity mirrors, and (3) consumption of the energy to molecular rotation motion in the SRS process. However, the main loss might arise from mismatching between the transverse mode of the input beam and the cavity mode. Thus we believe that the output power will be increased by improvements made in mode matching using advanced techniques.

An AC trace of the multifrequency emissions from the Raman cavity clearly showed an interferometric fringe and an undulating envelope that changed periodically, as shown in Fig. 3(a). The spectrum of the measured output beam is also shown in Fig. 3(b).¹⁸ This envelope in the AC trace suggests that the temporal waveform of the output beam has a pulselike structure whose intensity is periodically modulated. The period of the fringe was determined

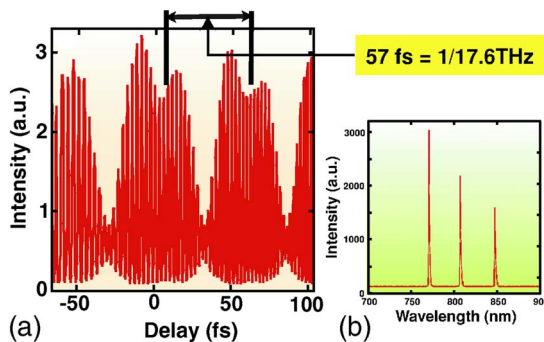


Fig. 3. (Color online) (a) Autocorrelation trace of an output beam from the Raman cavity. (b) The spectrum of the measured beam is also shown. The longitudinal mode contributing to the Stokes emissions was different from those shown in Fig. 2(a), causing the change of the output spectrum.

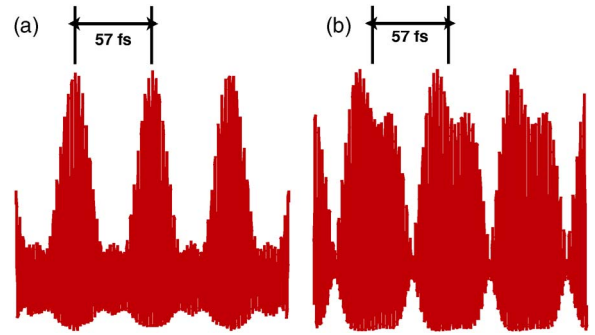


Fig. 4. (Color online) Calculated autocorrelation traces from the spectrum shown in Fig. 3(a). (a) The case in which two replica pulses have the same envelope. (b) Additional GDD arising from a silica plate is provided to only one replica pulse.

by the multiplicative inverse of the central frequency for the whole output spectrum. This confirmed the period of the periodic structure of the envelope as ~ 57 fs, which corresponds to the multiplicative inverse of the rotational Raman shift frequency ($=17.6$ THz). This clearly suggests that the temporal waveform of the output beam is modulated as a result of coherent superposition of the pump and the Stokes emissions. It should be pointed out that we generated a pulse train with a repetition rate of 17.6 THz ($\sim 1/57$ fs), which is, to our knowledge, the fastest repetition rate achieved for a CW optical pulse train. The AC trace shown in Fig. 3(a) has an asymmetric structure, which should not be observed in a typical AC trace, for the zero-delay time. This type of structure can be observed in an autocorrelator when waveforms of two replica pulses divided by a beam splitter in an autocorrelator are different. In the present autocorrelator, we used a one-side-coated silica plate with 3 mm thickness as a beam splitter. This configuration leads to a double pass of a beam through the silica substrate for just one replica pulse, resulting in distortion of the waveform for the replica due to additional group delay dispersion (GDD). To estimate the quantity of this effect, we calculated waveforms and their correlation traces under the assumption that an additional GDD of 150 fs², which is equivalent to that of a silica plate with a thickness of $3 \times \sqrt{2}$ mm, was provided to only one replica. Providing the same initial phase for all frequency components, correlation traces without and with an additional GDD for one replica are shown in Figs. 4(a) and 4(b), respectively. The trace shown in Fig. 4(b) is in good agreement with the experimental result shown in Fig. 3, strongly suggesting that the asymmetric structure is caused by the GDD arising from the substrate used as a beam splitter. These results, however, suggest that the use of a pair of beam splitters in a back-to-back configuration¹⁹ and suitable adjustment of a phase relationship among these three lines will lead to an AC trace with a symmetric shape as shown in Fig 4(a).

It should, however, also be noted that we could not observe a stable CW-based THz pulse train under the phase-locking condition, even when the phase relationship was completely adjusted. The reason for this can be explained as follows: For the complete phase-locking condition, the frequency separation between the pump and

S1 ($\Delta\nu_{p-s1}$) must be exactly identical to that between S1 and S2 ($\Delta\nu_{s1-s2}$):

$$\Delta\nu_{p-s1} = \Delta\nu_{s1-s2}. \quad (1)$$

The frequency of S1 is determined by the longitudinal mode of the cavity within the profile of the Raman gain that is located at the frequency separation of 17.6 THz from the frequency of the pump beam and has an ~ 1 GHz bandwidth at a pressure of 10 atm. The frequency of S2 is also determined, in a similar manner, by the frequency of the longitudinal mode of the cavity within the Raman gain profile for the S2 emission (see Fig. 5); namely, for the complete phase-locking condition, the frequency separations between the longitudinal modes for the generation of S1 and S2 must be exactly identical. The frequency separation between adjacent longitudinal modes (free spectral range, FSR) can be expressed as follows:

$$\text{FSR}(\lambda) = \frac{c}{2L} \cdot \frac{1}{n(\lambda) - \lambda[dn(\lambda)/d\lambda]}, \quad (2)$$

where λ is the wavelength, c is the velocity of light, L is the length of the cavity, and $n(\lambda)$ is the refractive index of a medium in the cavity as a function of λ . This equation indicates that the frequency separation between the adjacent longitudinal modes in the cavity cannot be the same value unless the refractive index of the medium is independent of the wavelength. The dispersion of the gaseous hydrogen in the Raman cavity cannot be negligible, even when the dispersion of the cavity mirrors may be assumed to be sufficiently small. We estimated the difference between $\Delta\nu_{p-s1}$ and $\Delta\nu_{s1-s2}$ to be ~ 7 MHz at a hydrogen pressure of 1 atm.²⁰ This indicates that the phase relationship among the emission lines deviated gradually as time passed and that the synthesized waveform also changed at a frequency of ~ 7 MHz.

Wavelength dependence of the refractive index $n(\lambda)$ of a medium is determined by the group velocity dispersion (GVD), which is the second-order derivative of the propagation constant, $k=n(\omega)\omega/c$, with respect to ω . The total GDD ($=\text{GVD} \times L$) in the cavity is determined by the sum of the GDDs in the gaseous Raman medium and the cavity mirrors. Therefore the $n(\lambda)$ can be canceled out by controlling the total GDD in the cavity to be zero. This is easily achieved using mirrors with negative dispersion (negative dispersion mirror, NDM) for the cavity component since the dispersion of the Raman medium is always

positive. An advanced NDM coated by ion-beam sputtering has a reflectivity larger than 99.95% over a frequency range larger than 50 THz with a loss of ~ 10 ppm (parts per million). When $L=8$ cm, the GDD of gaseous hydrogen at a pressure of 10 atm is ~ 10 fs² at the wavelength of the Stokes emission (806.5 nm). A NDM with this GDD value can be easily designed and manufactured by existing state-of-the-art technology. Use of a cavity consisting of such GDD-managed mirrors will lead to a phase-locking operation for the generation of a stable CW-THz pulse train, although the high-order terms of the refractive index may be a problem for a phase-locking operation over broader spectral ranges in this approach.²¹ We also should point out that complete compensation for the dispersion will lead to linear dependence in the propagation constant on the frequency. This means that the phase mismatching, Δk , in a parametric FWM process among three emissions becomes essentially zero.²² Since this FWM has no threshold and occurs more efficiently than SRS under phase-matching conditions, i.e., $\Delta k=0$, this will provide a useful means for the generation of a seed to strongly enhance Raman emission and for the stable phase-locked operation of the CW-THz pulse train.¹¹

4. CONCLUSIONS

We first demonstrated CW multifrequency generation arising from a high-finesse cavity filled with molecular hydrogen through a cascade process of stimulated Raman scattering (SRS). Using a highly sensitive autocorrelator, we observed a 17.6 THz pulselike intensity modulation caused by the coherent superposition of multifrequency CW emissions. We also pointed out that the phase-locked operation for the generation of a CW-THz pulse train is prevented due to the difference in the frequency separation between the adjacent emission lines, which can be attributed to intracavity dispersion. We are convinced that a phase-locked operation will be achieved using a pair of mirrors with negative dispersion as components of the Raman cavity.

ACKNOWLEDGMENTS

This research was supported by the Grants-in-Aid for Scientific Research and the 21st Century COE Program from the Ministry of Education, Culture, Science, Sports, and Technology of Japan.

Corresponding author S.-i. Zaitsu can be reached by e-mail at s-zaitsu@cstf.kyushu-u.ac.jp.

REFERENCES AND NOTES

1. B. B. Hu and M. G. Nuss, "Imaging with terahertz waves," *Opt. Lett.* **20**, 1716–1718 (1995).
2. A. Hasegawa, "Ultrahigh-speed optical communications," *Phys. Plasmas* **8**, 1763–1773 (2001).
3. D. Cotter, R. J. Manning, K. J. Blow, A. D. Ellis, A. E. Kelly, D. Nasset, I. D. Phillips, A. J. Poustie, and D. C. Rogers, "Nonlinear optics for high-speed digital information processing," *Science* **286**, 1523–1528 (1999).
4. S. Arahira, S. Oshiba, Y. Matsui, T. Kunii, and Y. Ogawa, "Terahertz-rate optical pulse generation from a passively mode-locked semiconductor laser diode," *Opt. Lett.* **19**, 834–836 (1994).

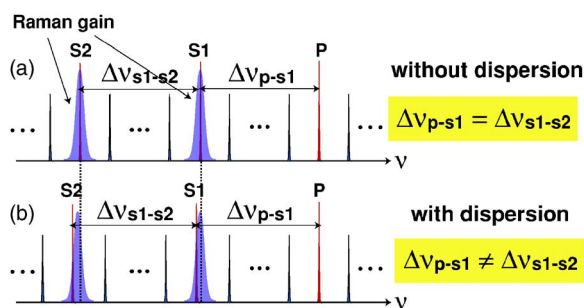


Fig. 5. (Color online) Longitudinal modes of the optical cavity (a) without and (b) with intracavity dispersion. The profiles of the Raman gain and the modes that contribute to the Raman lasing are also shown.

5. D. A. Yanson, M. W. Street, S. D. McDougall, I. G. Thayne, and J. H. Marsh, "Terahertz repetition frequencies from harmonic mode-locked monolithic compound-cavity laser diodes," *Appl. Phys. Lett.* **78**, 3571–3573 (2001).
6. M. Hyodo, K. S. Abedin, and N. Onodera, "Fourier synthesis of 1.8-THz optical-pulse trains by phase locking of three independent semiconductor lasers," *Opt. Lett.* **26**, 340–342 (2001).
7. Y. Ozeki, S. Takasaka, J. Hiroishi, R. Suguzaki, T. Yagi, M. Sakano, and S. Namiki, "Generation of 1 THz repetition rate, 97 fs optical pulse train based on comb-like profiled fibre," *Electron. Lett.* **41**, 1048–1050 (2005).
8. S. E. Harris and A. V. Sokolov, "Subfemtosecond pulse generation by molecular modulation," *Phys. Rev. Lett.* **81**, 2894–2897 (1998).
9. M. Y. Shverdin, D. R. Walker, D. D. Yavuz, G. Y. Yin, and S. E. Harris, "Generation of a single-cycle optical pulse," *Phys. Rev. Lett.* **94**, 033904 (2005).
10. M. Katsuragawa, K. Yokoyama, T. Onose, and K. Misawa, "Generation of a 10.6-THz ultrahigh-repetition-rate train by synthesizing phase-coherent Raman-sidebands," *Opt. Express* **13**, 5628–5634 (2005).
11. K. Shinzen, Y. Hirakawa, and T. Imasaka, "Generation of highly repetitive optical pulses based on intracavity four-wave Raman mixing," *Phys. Rev. Lett.* **87**, 223901 (2001).
12. K. Ihara, C. Eshima, S. Zaitsu, S. Kamitomo, K. Shinzen, Y. Hirakawa, and T. Imasaka, "Molecular-optic modulator," *Appl. Phys. Lett.* **88**, 074101 (2006).
13. J. K. Brasseur, K. S. Repasky, and J. L. Carlsten, "Continuous-wave Raman laser in H_2 ," *Opt. Lett.* **23**, 367–369 (1998).
14. T. Hattori, Y. Kawashima, M. Daikoku, H. Inoue, and H. Nakatsuka, "Autocorrelation measurement of femtosecond optical pulses based on two-photon photoemission in a photomultiplier tube," *Jpn. J. Appl. Phys., Part 1* **39**, L809–L811 (2000).
15. G. S. He and S. H. Liu, *Physics of Nonlinear Optics* (World Scientific, 1999).
16. R. W. Minck, E. E. Hagenlocker, and W. G. Rado, "Stimulated pure rotational Raman scattering in deuterium," *Phys. Rev. Lett.* **17**, 229–231 (1966).
17. K. S. Repasky, J. K. Brasseur, L. Meng, and J. L. Carlsten, "Performance and design of an off-resonant continuous-wave Raman laser," *J. Opt. Soc. Am. B* **15**, 1667–1673 (1998).
18. The longitudinal modes contributing to the generation of the Stokes emissions differed between the spectrum shown in Fig. 2(a) and that shown in Fig. 3(b). Owing to the bandwidth of a Raman gain, the efficiency for both Stokes emissions varied depending on the related longitudinal modes even when the pump power was constant.
19. C. Spielmann, L. Xu, and F. Krausz, "Measurement of interferometric autocorrelations: comment," *Appl. Opt.* **36**, 2523–2525 (1997).
20. We used the formula described in E. R. Peck and S. Huang, "Refractivity and dispersion of hydrogen in the visible and near infrared," *J. Opt. Soc. Am.* **67**, 1550–1554 (1977) to calculate the difference between $\Delta\nu_{p-s1}$ and $\Delta\nu_{s1-s2}$. At the wavelength of P (770.0 nm), $n=1.000137506$, and $dn/d\lambda=-4.67008$. At the wavelength of S1 (806.5 nm), $n=1.000137345$, and $dn/d\lambda=-4.04611$. At the wavelength of S2 (846.5 nm), $n=1.000137198$ and $dn/d\lambda=-3.50354$.
21. We estimate that the suppression of the difference between $\Delta\nu_{p-s1}$ and $\Delta\nu_{s1-s2}$ below the linewidth of a longitudinal mode of a high-finesse cavity (~ 500 kHz) over a range of 70 THz, which includes five Raman emissions, needs the third-order dispersion to be less than 0.5 fs^3 .
22. R. W. Boyd, *Nonlinear Optics* (Academic, 2003).